On Three Levels

Micro-, Meso-, and Macro-Approaches in Physics

Edited by

Mark Fannes

Christian Maes

and

André Verbeure

Katholieke Universiteit Leuven
Leuven, Belgium

Plenum Press (1994)
New York and London
Published in cooperation with NATO Scientific Affairs Division

MULTIFRACTAL PROPERTIES OF DISCRETE STOCHASTIC MAPPINGS

U. Behn[1], J.L. van Hemmen[2], R. Kühn[3], A. Lange[1], and V.A. Zagrebnov[4]

1. Institut für Theoretische Physik, Universität Leipzig
   D-04109 Leipzig, Germany
2. Physik-Department, TU München
   D-85747 Garching, Germany
3. Institut für Theoretische Physik, Universität Heidelberg
   D-69120 Heidelberg, Germany
4. Instituut voor Theoretische Fysica, Katholieke Universiteit Leuven
   B-3001 Leuven, Belgium

In different fields of statistical physics, such as 1d random field Ising models (RFIM) and neural networks, there appear discrete stochastic mappings of the form

$$x_n = f_n(x_{n-1}) \tag{1}$$

where $f_n(x)$ is chosen with equal probability from two functions $f_\sigma(x)$, $\sigma = +$ or $-$, and $0 < f'_\sigma(x) \leq 1$. The dynamics is nonchaotic and, in a region of physical parameters, converges to a *strange* (fractal) attractor as may be visualized in Fig. 1. The mapping generates an invariant measure which undergoes, as parameters are changed, qualitative transitions, for instance, a transition from thin to fat multifractal.

To be specific, for the 1d RFIM[1–7] with random field h_n on lattice site n taking the values $h_n = h_0 \pm h$, the effective local random field is generated by (1) choosing $f_n(x) = h_n + A(x)$, where $A(x) = (2\beta)^{-1} \ln [\cosh \beta(x + J)/ \cosh \beta(x - J)]$. β and J are inverse temperature and exchange, respectively. In neural networks (1) is the learning rule for a forgetful memory[7,8] choosing $f_n(x) = \tanh(\varepsilon_n + x)$. Here x_{n-1} is the synaptic coupling between two neurons, say i and j, and $\varepsilon_n = \pm\varepsilon$ is the weight added through the learning of the nth random pattern. The analytic formalism for both models is the same. In presenting numerical results we restrict ourselfes here to the case of the learning rule which has only *one* parameter ε. For details the reader is referred to Refs. 6 and 8.

On Three Levels, Edited by M. Fannes *et al.*,
Plenum Press, New York, 1994

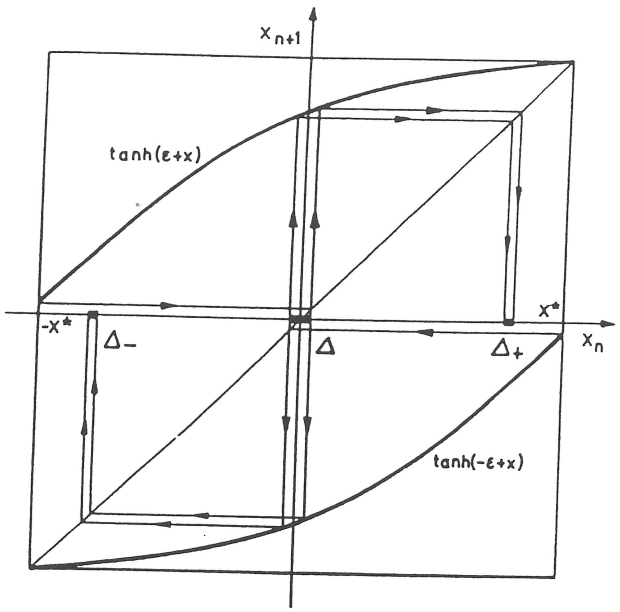

Figure 1. Discrete stochastic mapping in the case of nonoverlapping bands. Only gaps of first (Δ) and second (Δ_σ) generations are indicated.

The Frobenius-Perron equation corresponding to (1) reads

$$p_n(x) = \int dy\, p_{n-1}(y) \frac{1}{2} \sum_{\sigma=\pm} \delta(x - f_\sigma(y)). \tag{2}$$

The fixed point of (2) gives the invariant measure which is a multifractal. To evaluate (2) it is advantageous to introduce a symbolic dynamics which encodes the result of the mapping (1) by the sequence of signs characterizing the history of the dynamical system. We denote the result of the nth iteration of (1) by

$$x_{\{\sigma\}_n,y} = f_{\sigma_n}(f_{\sigma_{n-1}}(\ldots f_{\sigma_1}(y) \ldots)), \tag{3}$$

where $\{\sigma\}_n$ is the sequence of n signs $+$ or $-$ corresponding to the given realization of the random sequences $\{h_n\}$ or $\{\epsilon_n\}$. The result of infinitely many iterations is denoted by $x_{\{\sigma\}}$ where $\{\sigma\}$ symbolizes an infinite sequence of signs. Infinitely many iterations with the *same* function, say f_+, leads to a fixed point denoted by $x_{\{+\}}$. It is easy to see that $x_{\{+\}}$ and $x_{\{-\}}$ are the boundaries of the support of the invariant measure. For the learning rule and the RFIM in the case $h_0 = 0$ the measure is symmetric so that $x_{\{+\}} = -x_{\{-\}}$. The iteration of (2) starting with the initial measure $p_0(x)$ generates a probability measure which may be also encoded by symbolic dynamics. In the first step we obtain two bands $p_\sigma(x)$ living on the intervals $I_\sigma = [x_{\sigma\{-\}}, x_{\sigma\{+\}}]$

$$p_\sigma(x) = p_0(y_{\sigma,x}) [2f'_\sigma(y_{\sigma,x})]^{-1} \quad \text{for } x \in I_\sigma\,, \qquad \sigma = \pm \tag{4}$$

where $y_{\sigma,x} = f_\sigma^{-1}(x)$ denotes the preimage of x for the mapping f_σ. Each band generates in the next step two new bands so that in the nth generation the measure consists of

2^n bands,

$$p_{\{\sigma\}_n}(x) = p_0(y_{\{\sigma\}_n,x}) \prod_{\nu=1}^{n} \left[2f'_{\sigma_\nu}(y_{\{\sigma\}_\nu,x})\right]^{-1} \qquad \text{for } x \in I_{\{\sigma\}_n} \tag{5}$$

labeled by the 2^n possible configurations $\{\sigma\}_n$. The notations $y_{\{\sigma\}_n,x}$ and $I_{\{\sigma\}_n}$ are obvious. Thus the measure in the nth iteration may be represented as $p_n(x) = \sum_{\{\sigma\}_n} p_{\{\sigma\}_n}(x)$. This explicit representation is helpful to investigate the qualitative behaviour of the measure and to calculate generalized scaling exponents.

The two bands in the first step may overlap or not and correspondingly the *support* of the measure is the whole interval $I = [x_{\{-\}}, x_{\{+\}}]$ or a fractal with the topology of a Cantor set. The *measure* constitutes in the former case a *fat* multifractal (Fig. 2a-c) and in the latter case a *thin* multifractal (Fig. 2d). In the case of the learning rule the condition of zero overlap defines the critical parameter $\varepsilon_c^{(1)} \simeq 0.957$.

The histograms generated by numerical simulation of (1) (or alternatively by numerical solution of (2)) reveal that, depending on physical parameters, there are qualitative changes in the behaviour of the measure at the boundaries of the support, cf. Fig. 2. The invariant measure for the membrane potential in a single-neuron model [9] shows a similar behaviour. These changes can be analyzed exploiting that the preimage of the fixed point is the fixed point itself. For example we consider the right boundary $x_{\{+\}} = x^*$. In the nth iteration we obtain from (5) for the rightmost band

$$p_{\{+\}_n}(x^*) \sim \left[2f'_+(x^*)\right]^{-n} \tag{6}$$

which goes in the limit $n \to \infty$ to ∞ or 0, unless $f'_+(x^*) = 1/2$. The latter condition separates two parameter regions in which the invariant measure at its right boundary diverges (Fig. 2c, d) or goes to zero (Fig. 2a,b), respectively.

To investigate the scaling behaviour of the coarse grained measure at the boundaries of the support we consider

$$P(l) = \lim_{n\to\infty} P_n(l) = \lim_{n\to\infty} \int_{x^*-l}^{x^*} dx\, p_n(x) \tag{7}$$

which is expected to behave like $P(l) \sim l^\alpha$ as $l \to 0$ with the scaling exponent α to be determined. In the *scaling limit* we chose $l = l_n \sim \left[f'_+(x^*)\right]^n \to 0$ as $n \to \infty$ which ensures that only the righmost band $p_{\{+\}_n}(x)$ contributes to (7). Application of (5) and expansion near the fixed point leads to the scaling law[8]

$$P_n(l) = \int_{x^*-l}^{x^*} dx\, p_{\{+\}_n}(x) \sim l^\alpha\,, \qquad \alpha = -\frac{\ln 2}{\ln f'_+(x^*)}\,. \tag{8}$$

The coarse grained density at the boundaries of the support $\tilde{p}(l) = P(l)/l$ scales as $l^{\alpha-1}$, i.e., it goes to ∞ or 0 unless $f'_+(x^*) = 1/2$ as already found from (6). The left derivative of the coarse grained density at x^* scales as $l \to 0$ like

$$-\partial_l \tilde{p}(l) \sim -(\alpha-1) l^{\alpha-2}\,. \tag{9}$$

Correspondingly, there are parameter regions in which the left derivative of the density goes to zero (for $\alpha > 2$, i.e., $f'_+(x^*) > 1/\sqrt{2}$), to $-\infty$ (for $2 > \alpha > 1$, i.e., $1/\sqrt{2} > f'_+(x^*) > 1/2$), or to ∞ (for $1 > \alpha$, i.e., $1/2 > f'_+(x^*)$). This explains analytically the qualitative changes found in the numerical simulations, cf. Fig. 2a-c. In the case of the learning rule the above conditions for qualitative changes define the critical parameters $\varepsilon_c^{(2)} \simeq 0.174$ and $\varepsilon_c^{(3)} \simeq 0.064$.

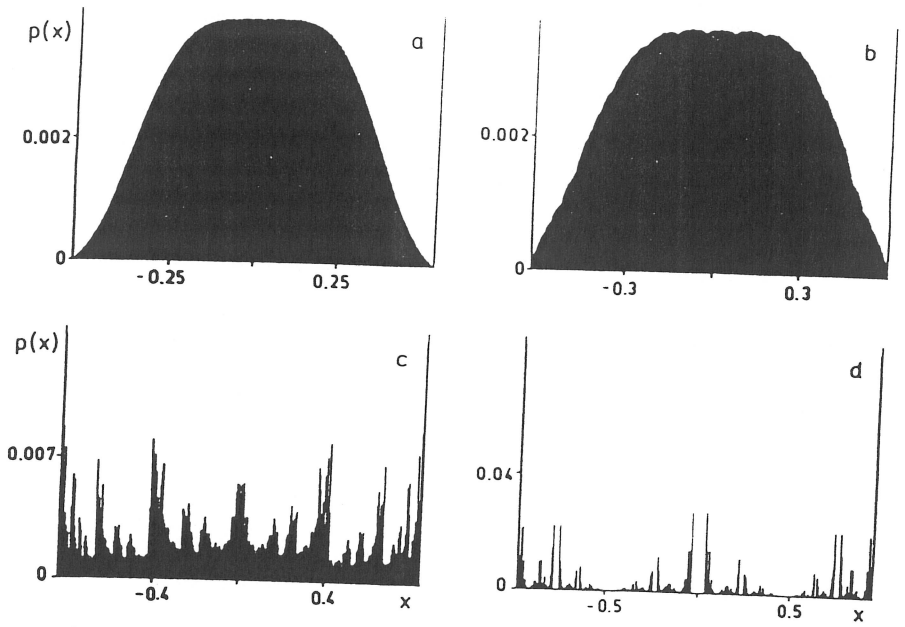

Figure 2. Qualitatively different shapes of invariant maesures. In (a)-(d) we have $\epsilon = 0.05$, 0.1, 0.4, and 1.0, respectively. The measure at the boundaries of the support is either zero, (a) and (b), or infinite, (c) and (d). The former case is further distinguished by the derivative of the outmost bands at the boundaries of the support, which either vanishes (a) or diverges (b). The multifractal measure in (a)-(c) covers the whole interval (fat fractal), whereas in (d) it is a thin fractal. The histograms are calculated by a digital simulation of a trajectory of length 10^9. Note the different scales on both axes.

After examining the behaviour of the invariant measure at the boundaries of its support we turn to characterize the scaling behaviour of the invariant measure on the *whole* support by generalized fractal dimensions,

$$D_q = \frac{1}{q-1} \lim_{l \to 0} \frac{\ln \sum_{i=1}^{N(l)} P_i^q}{\ln l} \,. \tag{10}$$

Here the sum runs over all $N(l)$ nonoverlapping cells of length l used to cover the support, and P_i denotes the total weight of the measure on cell i. For $q = 0$, 1, 2 (10) gives the Hausdorff, information, and correlation dimension, respectively. The limiting values D_∞ and $D_{-\infty}$ characterize the most dominating and most rare parts of the multifractal, respectively.

In cases, where the cells at the boundary of the support correspond to the most rare or most dominant events, our previous scaling analysis leads to $D_{-\infty} = \alpha$ or $D_\infty = \alpha$ with α given in (8).

To compute the fractal dimensions in general, it is advantageous to use instead of the equipartion of the support the *natural* partition generated by the mapping itself. In the thermodynamic formalism[10], the partition function $\Gamma_n(q,\tau) = \sum_i P_i^q / l_i^\tau$ calculated

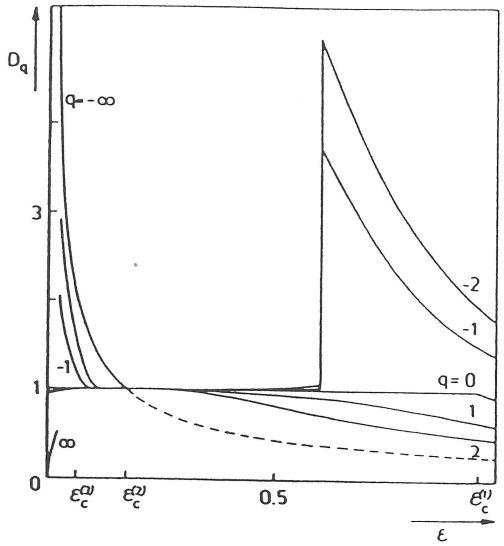

Figure 3. Generalized fractal dimensions D_q of the invariant measure corresponding to the learning rule, for $q = 0, \pm 1, \pm 2$. The most remarkable feature is that the width of the multifractal spectrum becomes narrow near $\varepsilon_c^{(2)}$ where the measure at the boundaries of the support jumps from zero to infinity. For $\varepsilon < \varepsilon_c^{(2)}$, $D_{-\infty}(\varepsilon)$ is also displayed. For $\varepsilon > \varepsilon_c^{(2)}$, the dashed line shows the scaling exponent α of the right(left)most band, which approaches $D_\infty(\varepsilon)$ as ε becomes large. For $\varepsilon \to 0$, we have drawn $D_\infty(\varepsilon) \to 0$ only schematically.

with the natural partition in a given generation of the hierarchy goes to zero or to infinity as $n \to \infty$ unless $\tau = (q-1)D_q$. This can be used to determine the D_q which can be shown[11] to agree with those determined from (10).

The natural partition is for the case of nonoverlapping bands given by the 2^n images $I_{\{\sigma\}_n}$ of the initial interval I, each carrying the same total measure 2^{-n}. For overlapping bands $I_{\{\sigma\}_n}$ where the support of the measure is the whole interval we use the 2^{n+1} endpoints of the $I_{\{\sigma\}_n}$ for repartioning into $2^{n+1}-1$ nonoverlapping new intervals[6,8]. Each of these new intervals in general carries weight from several bands. We determined the D_q by solving $\Gamma_n(\tau) - \Gamma_{n-1}(\tau) = 0$ $(n = 10, \ldots, 15)$ as an eigenvalue equation[12] for τ.

Qualitatively, the behaviour of the generalized dimensions shown in Fig. 3 can be understood as follows. The tails of the measure at the boundaries of the support determine $D_{-\infty}(\varepsilon)$ for $\varepsilon < \varepsilon_c^{(2)}$. In particular, $D_{-\infty}(\varepsilon)$ diverges, as $\varepsilon \to 0$. In the same limit, the mass of the distribution concentrates at the center of the support in a δ-function like fashion, so that $D_\infty(\varepsilon)$ decreases to zero as $\varepsilon \to 0$. In the opposite limit, $\varepsilon \to \infty$, the invariant measure is a *thin* fractal, collapsing into two δ-functions at the endpoints of the support. This means that all fractal dimensions approach zero, implying that the width of the spectrum of fractal dimensions approaches zero, too.

Now we look at the fate of the multifractal as ε decreases from large to small values. For still large ε, the fractal is thin and most bins are empty at any resolution. With decreasing ε, the fractal becomes more dense, and all fractal dimensions increase.

If the gaps close, the fractal becomes fat, and $D_0 = 1$ for all $\varepsilon < \varepsilon_c^{(1)}$. However there are still very deep valleys and high peaks on all scales that cause D_q for $q > 0$ or $q < 0$ to be smaller or larger than D_0, respectively. Upon further decrease of ε the D_q for $q < 0$ decrease drastically and reach values close to 1, which announces that a dense nonfractal "background" on the whole support has emerged. Still, superimposed on this background, there are peaks on all scales, so that $D_q < 1$ for $q > 0$. At $\varepsilon_c^{(2)}$, the behaviour of the measure at the boundaries of the support changes qualitatively, $\tilde{p}(\pm x^*)$ jumps from ∞ to zero as ε is decreased through this critical value, and $D_{-\infty} = 1$. For $\varepsilon_c^{(3)} < \varepsilon < \varepsilon_c^{(2)}$, there are tails decreasing to zero with infinite slope as $x \to \pm x^*$. At $\varepsilon_c^{(3)}$ there is yet another qualitative change, the slope jumps from ∞ to zero, i.e., $D_{-\infty} = 2$. The scaling behaviour of this slope determines $D_{-\infty}$ as discussed earlier.

The 1d RFIM shows a similar behaviour of the invariant measure varying h for suitably choosen nonzero temperature and homogeneous field. Since there the parameter space is three dimensional the behaviour of fractal dimensions exhibits a richer phenomenology including discontinuous transitions[6].

Transitions in the behaviour of invariant measures (or their projections) generated by iterated function systems have been recently discussed in a different context[13].

REFERENCES

1. G. Györgyi and P. Rujàn, Strange attractors in disordered systems, *J. Phys. C*, **17**, 4207 (1984).
2. U. Behn and V.A. Zagrebnov, One-dimensional random field Ising model and discrete stochastic mappings, *J. Stat. Phys.*, **47**, 939 (1987); One-dimensional Markovian field Ising model: Physical properties and characteristics of the discrete stochastic mapping, *J. Phys. A*, **21**, 2151 (1988); Comment on "Random-field Ising model as a dynamical system", *Phys. Rev. B*, **38**, 7115 (1988); U. Behn, V.B. Priezzhev, and V.A. Zagrebnov, One dimensional random field Ising model: Residual entropy, magnetization, and the "perestroyka" of the ground state, *Physica A*, **167**, 457 (1990).
3. P. Szépfalusy and U. Behn, Calculation of a characteristic fractal dimension in the one-dimensional random field Ising model, *Z. Phys. B*, **65**, 337 (1987).
4. J. Bene and P. Szépfalusy, Multifractal properties in the one-dimensional random field Ising model, *Phys. Rev. A*, **37**, 1702 (1988); J. Bene, Multifractal properties of a class of non-natural measures as an eigenvalue problem, *Phys. Rev. A*, **39**, 2090 (1988).
5. T. Tanaka, H. Fujiska, and M. Inoue, Free-energy fluctuations in a one-dimensional random Ising model, *Phys. Rev. A*, **39**, 3170 (1989); Scaling structures of free-energy fluctuations in a one-dimensional dilute Ising model, *Progr. Theor. Phys.*, **84**, 584 (1990).
6. U. Behn and A. Lange, 1D random field Ising model and nonlinear dynamics, *in*: "From Phase Transition to Chaos," G. Györgyi, I. Kondor, L. Sasvári, and T. Tél, eds., World Scientific, Singapore (1992).
7. J.L. van Hemmen, G. Keller, and R. Kühn, Forgetful memories, *Europhys. Lett.*, **5**, 663 (1988).
8. U. Behn, J.L. van Hemmen, R. Kühn, A. Lange, and V.A. Zagrebnov, Multifractality in forgetful memories, *Physica D*, **68**, (1993).
9. P.C. Bressloff, Analysis of quantal synaptic noise in neural networks using iterated function systems, *Phys. Rev. A*, **45**, 7549 (1992).
10. T.C. Halsey, M.H. Jensen, I. Procaccia, and B.I. Shraiman, Fractal measures and their singularities: The characterization of strange sets, *Phys. Rev. A*, **33**, 1141 (1989).
11. H.B. Lin, "Elementary Symbolic Dynamics and Chaos in Dissipative Systems," World Scientific, Singapore (1989).
12. M.J. Feigenbaum, I. Procaccia, and T. Tél, Scaling properties of multifractals as eigenvalue problem, *Phys. Rev. A*, **39**, 5359 (1989).
13. G. Radons, H.G. Schuster, and D. Werner, Fractal measures and diffusion as results of learning in neural networks, *Phys. Lett. A*, **174**, 293 (1993); G. Radons, A new transition for projections of multifractal measures and random maps, *J. Stat. Phys.*, **72**, 227 (1993).